Proceedings of the 20th International Conference on Soil Mechanics and Geotechnical Engineering– Rahman and Jaksa (Eds)

Behavior of a rockfill material with the independent variation of the stress Lode's angle

Propriétés des matériaux de remblai rocheux avec variation indépendante de l'angle de contrainte Lord

Yuefeng Zhou, Jiajun Pan, Zhanlin Cheng & Yongzhen Zuo
Key Laboratory of Geotechnical Mechanics and Engineering of Ministry of Water Resources, Changjiang River Scientific Research Institute, Wuhan, China, zhou.yuefeng@163.com

ABSTRACT: The behavior of a rockfill material with the independent variation of the stress Lode's angle is investigated via a series of stress-path tests using a self-developed large-scale true triaxial apparatus. In each test, the stress Lode's angle was designed to increase and then decrease between -30° and 30° twice under the condition of constant effective mean principal stress p and constant deviatoric stress q. The stress path is within one-sixth stress deviatoric plane, and represents the whole plane due to its symmetry. Experimental results show that soil deformation occurs under the condition of constant mean and deviatoric stresses. Initial slope of deviatoric strain curve increases as the stress ratio q/p grows. Hystereses are observed for the deviatoric strain, the volumetric strain, and the strain Lode's angle, the last of which is needed to determine strain state in the strain space. Being affected by the initial stress ratio q/p, the rockfill material could reach failure state with the increasing stress Lode's angle. Based on strain deviatoric plane analysis, the rockfill material shows non-coaxial characteristics prior to failure, and tends to be coaxial at failure state. The material dilatancy following the above path is finally analyzed.

RÉSUMÉ : Les caractéristiques des matériaux de remblai rocheux soumis à un changement indépendant de l'angle de contrainte - lode ont été étudiées à l'aide d'une série d'essais de cheminement de contrainte à l'aide d'un instrument triaxial réel à grande échelle auto - développé. Pour chaque essai, l'angle de contrainte Lord est conçu pour augmenter puis diminuer deux fois entre - 30° et 30° à la contrainte principale moyenne effective constante p et à la contrainte de biais constante q. La trajectoire de contrainte est située dans le plan de déviation d'un sixième de la contrainte et, en raison de sa symétrie, elle représente l'ensemble du plan.Les résultats des essais montrent que la déformation du sol se produit dans des conditions de contrainte moyenne et de contrainte partielle constante. La pente initiale de la courbe de déformation partielle augmente avec l'augmentation du rapport de contrainte q/p. On a observé des hystérèses de déformation partielle, de déformation volumique et d'angle de déformation - lode, le dernier hystérèse étant utilisé pour déterminer l'état de déformation dans l'espace de déformation. Sous l'influence du rapport de contrainte initial q/p, le remblai rocheux atteint l'état de rupture avec l'augmentation de l'angle de la veine de contrainte. Sur la base de l'analyse du plan partiel de déformation, les matériaux de remblai rocheux présentent des caractéristiques non coaxiales avant la rupture et tendent à être coaxiaux à l'état de rupture. Enfin, le gonflement par cisaillement du matériau le long de la trajectoire ci - dessus est analysé.

KEYWORDS: true triaxial test; Lode's angle; stress path; deviatoric plane; rockfill material; dilatancy.

1 INTRODUCTION

Rockfill material is utilized in dam construction whose mechanical behavior greatly affects the compatible deformation of dam body. It is considered to have intrinsic similar properties with sand as both are cohesionless materials being affected by factors such as mineral composition, particle size, shape, gradation, relative density (Honkanadavar and Sharma, 2016). Despite rockfill material was commonly investigated on an extension of sand behavior, its maximum diameter in dam construction can achieve one meter and needs to be reduced when laboratory test is required. To date, considerable studies using conventional triaxial tests or plane strain tests have been performed to investigate the behavior of rockfill material. However, rockfill material is commonly under general stress conditions and experiences complex stress paths in the periods of dam construction and reservoir impoundment (Xiao et al. 2011). In order to study its behavior, researchers have paid great efforts in the development of true triaxial apparatus with different specimen sizes (e.g., Lade and Wang 2001; AnhDan et al. 2006; Choi et al. 2008; Yin et al. 2010; Xiao et al. 2011; Cheng et al. 2015).

Dilatancy is the volume change observed in granular materials when they are subjected to shearing. The stress–dilatancy relation plays a significant role in modeling the behavior of granular material as it establishes the plastic flow rule in an elastoplastic constitutive model. Rowe (1962) proposed that dilatancy has a unique relation with q/p stress ratio and termed it as stress-dilatancy relation. On the basis of plastic work dissipation in triaxial condition, two forms of dilatancy equations were presented in Cam-clay model and Modified Cam-clay model (Wood 1990). Despite the above equations worked well for cohesive soils, it was noticed that the dilatancy of granular material is affected by density (Wan and Guo 1997; Guo et al. 2007; Taiebat and Dafalias 2008). With the concept of state parameter as basis, Li and Dafalias (2000) proposed a state-dependent dilatancy equation to consider a sand with different initial densities as the same material. Above equation promoted the great development of state-dependent critical state theory. Salim and Indraratna (2004) presented dilatancy for coarse granular soils with consideration of particle breakage. Above findings were majorly introduced based on experimental evidence under the triaxial condition. However, the dilatancy of rockfill material has not been sufficiently examined under general stress conditions, such as the stress path with different stress Lode's angle or intermediate principal stress ratio values. Xiao et al. (2011) presented a dilatancy equation under a general stress condition to shed light on the above issue. The stress-path dependent parameter in their equation still needs further clarification.

There are three independent stress components necessary to describe the stress state at a certain point in stress space. For example, the principal stresses components (σ_1, σ_2, σ_3), the stress

invariables (I_1, I_2, I_3), the generalized stresses components (p, q, b or θ_σ) etc. Previous studies on sand and clay have proved that the intermediate principal stress σ_2 has a great contribution to material behavior. However, its influence has largely been neglected when conducting geomechanical analysis in engineering practice. The popularity of the Mohr-Coulomb criterion can be partly attributed to the limitations of conventional triaxial testing. In most current soil's constitutive models, the mean principal stress p and the deviatoric stress q are utilized to deduce the volumetric and deviatoric strains in incremental form. A main issue which needs to be further revealed for the behavior of rockfill material under a general stress state is the effect of intermediate principal stress ratio b or the stress Lode's angle θ_σ, both of which are equivalent and contain the effect of σ_2 in the generalized stress framework. A series of representative findings are based on stress-path tests under constant σ_3 and constant b conditions. Issues such as shear strength, shear band, critical states line etc. are explored respectively (e.g., Lade and Wang 2001; AnhDan et al. 2006; Zhou et al. 2017). The above type of stress-path test can be conveniently performed via maintaining a constant effective confining pressure σ_3. However, it is difficult to evaluate the effect of b value on the stress-dilatancy behavior under such loading conditions, as the changing mean stress could exert influence as well (Xiao et al. 2015). With the development of geotechnical testing technique, stress-path tests under constant p and constant b conditions are carried out later. More reasonable soil behavior can be obtained as the stress path is within a fixed deviatoric plane (Ye et al. 2014). Meanwhile, it should be noticed that some theoretical or experimental evidences still clarified that the volumetric strain is affected by deviatoric stress as well (Indraratna et al. 1998; Li and Dafalias 2000).

If the influence of varying mean and deviatoric stresses on soil dilatancy could be eliminated, we can obtain further insight into soil behavior affected by the variation of the stress Lode's angle or the intermediate principal stress ratio. In the stress space, stress states with constant mean and deviatoric stresses have the same vector length from the origin and are along a circle in the same deviatoric plane (Shi et al. 2015). This article aims to reveal the behavior of a rockfill material with the independent variation of the stress Lode's angle, which so far has not been conferred sufficently from the experimental points of view. The experimental results and theoretical analyses should be vital towards developing a more comprehensive constitutive model.

2 TRUE TRIAXIAL TESTS

2.1 *Test apparatus*

A large-scale true triaxial apparatus (Fig. 1a) with a mixed rigid-flexible loading pattern developed by Cheng et al. (2015) was adopted in this study. The true triaxial apparatus adopts tall quadrilateral specimens with 300 mm length, 300 mm width and 600 mm height (Fig. 1b). The true triaxial apparatus includes six sets of loading and measuring systems, each of which contains a laser displacement transducer, a load cell and a hydro-cylinder. Two of them are in the vertical direction, and four in the lateral direction. In addition, the true triaxial apparatus includes the following components: a cell pressure transducer, a pore-water pressure transducer, an outer and an inner volumetric strain measuring component. The controlling system was designed to implement a certain user-defined stress path using stress transformation algorithms. The data acquisition system was developed to acquire electronic signals, and to transfer them into digital data for storage and analysis.

If the influence of varying mean stress and deviatoric stress on soil dilatancy could be eliminated, we can obtain further insight into soil behavior affected by the variation of the stress Lode's angle or the intermediate principal stress ratio. In the stress space, stress states with constant mean and deviatoric stresses have the same vector length from the origin and are along a circle in the same deviatoric plane (Shi et al. 2015). This article aims to reveal the behavior of a rockfill material with the independent variation of the stress Lode's angle, which so far has not been conferred sufficently from the experimental points of view. The experimental results and theoretical analyses should be vital towards developing a more comprehensive constitutive model. The loading pattern in a true triaxial test is introduced as follows. In the direction of minor principal stress, cell water pressure is exerted on a specimen as a flexible loading pattern. In the direction of major principal stress, vertical load is enforced by means of a pair of rigid platens at the top and the bottom of the specimen. In the direction of intermediate principal stress, lateral load is exerted on the specimen via a special low-friction loading platen technique. The low-friction loading platen is composed of a series of slide blocks, which transfer integral contact into distributed contact. The slide blocks are underlain by slight ball bearings and grooves, which can move laterally and vertically. In the loading process, the local deformation of a specimen occurs with movement of slide blocks. Rolling friction can substitute for sliding friction, leading to a considerable reduction in resistance (Cheng et al. 2015). Utilizing this apparatus, three unequal principal stresses can be enforced without the corner interference problem.

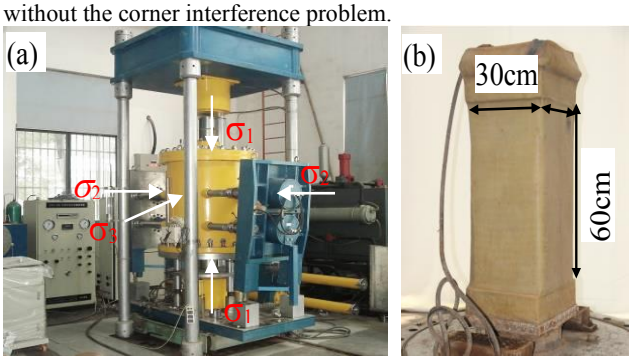

Figure 1 (a) The large-scale true triaxial apparatus and (b) its specimen

2.2 *Test material*

The rockfill material was obtained from a high core rockfill dam in western China. It was quarried by the means of slate blasting and crushing, whose particle shapes are angular and subangular. With consideration of specimen size, laboratory testing of prototype rockfill materials in dam construction is near imposible because of large particles. According to Specification on soil testing SL237-1999, particle size of the prototype rockfill material was reduced through the combination of parallel gradation technique and equivalent replacing technique and then adopted in laboratory (Fig. 2). The maximum particle diameter is 60 mm in true triaxial tests, suggesting that the maximum diameter ratio of particle to specimen is 1:5. Based on the results of index tests, the rockfill material has a specific gravity of 2.72. Minimum and maximum dry densities were also obtained as 1.620 g/cm3 and 2.134 g/cm3, respectively.

The rockfill material specimens were compacted in a split mould in four equal layers using the moist tamping technique. Based on the controlled dry density of 2.000g/cm3, the relative density and porosity were determined as 0.79 and 26.5%, respectively. In each layer, different components of rockfill material are mixed independently to ensure a relatively uniform composition.

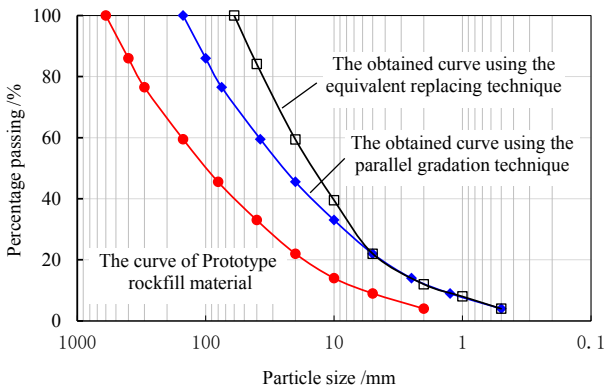

Figure 2. Particle size distribution curves of the rockfill material

2.3 *Test program*

As presented in Table 1, a total of three drained true triaxial tests (CPQ tests) were performed under constant mean effective principal stress and constant deviatoric stress conditions. The controlled mean stress is 0.4 Mpa, while the controlled deviatoric stresses are 0.4 Mpa, 0.5 Mpa and 0.6 Mpa, respectively. Firstly, a specimen was isotropically consolidated to the confining pressure 0.4 Mpa. Maintaining constant mean stress and constant b (=0), the specimen was then anisotropically consolidated to the designed values of the deviatoric stress, i.e. 0.4 Mpa, 0.5 Mpa and 0.6 Mpa, respectively. Thereafter, a specimen was subjected to the specified CPQ stress path below: maintaining constant mean and deviatoric stresses, the b value was increased from 0 to 1, and then decreased from 1 to 0; then repeat once. The stress Lode's angel θ_σ is fully associated with the intermediate principal stress ratio b and can be calculated below:

$$\tan\theta_\sigma = (2\sigma_2 - \sigma_1 - \sigma_3)/[\sqrt{3}(\sigma_1 - \sigma_3)] = (2b-1)/\sqrt{3} \quad (1)$$

According to eq. (1), the θ_σ value is between -30° and 30° with the b value ranging from 0 to 1. As demonstrated in Fig. 3, the stress paths are in the same deviatoric plane. According to the sequence of principal stresses, the stress deviatoric plane can be separated into six 60° sectors. The stress states and paths in the current study are within one-sixth stress deviatoric plane and represent the whole plane due to its symmetry (Fig. 3).

Table 1. Scheme of true triaxial tests

No.	p/MPa	q/MPa	b value	θ_σ /°	Test process
CPQ1	0.4	0.4	0~1	-30~30	Increasing and then decreasing b and θ_σ twice
CPQ 2	0.4	0.5	0~1	-30~30	Increasing and then decreasing b and θ_σ twice
CPQ 3	0.4	0.6	0~1	-30~30	Increasing b and θ_σ once

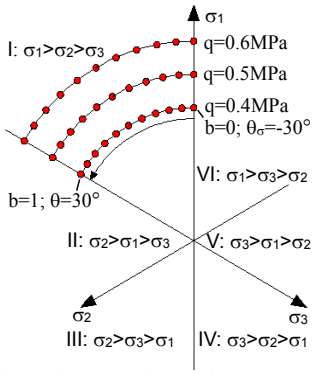

Figure 3. Stress paths in the stress deviatoric plane in constant p and q tests

The relationship between the principal stress components and the generalized stress components can be expressed as follows:

$$\sigma_1 = 2/3qsin(\theta_\sigma + 2/3\pi) + p \quad (2)$$

$$\sigma_2 = 2/3qsin\theta_\sigma + p \quad (3)$$

$$\sigma_3 = 2/3qsin(\theta_\sigma - 2/3\pi) + p \quad (4)$$

where σ_1, σ_2 and σ_3 are the major, intermediate and minor principal stresses, respectively.

The volumetric strain ε_v and the deviatoric strain ε_q can be calculated below:

$$\varepsilon_v = \varepsilon_1 + \varepsilon_2 + \varepsilon_3 \quad (5)$$

$$\varepsilon_q = \{2/9[(\varepsilon_1 - \varepsilon_2)^2 + (\varepsilon_1 - \varepsilon_3)^2 + (\varepsilon_2 - \varepsilon_3)^2]\}^{1/2} \quad (6)$$

where ε_1, ε_2 and ε_3 are the major, intermediate and minor principal strains, respectively.It should be noted that the term 'mean stress' is the short form of 'mean effective principal stress', and effective stress is generally considered in this article.

3 TEST RESULTS AND ANALYSIS

Taking the test CPQ1 with constant deviatoric stress q=0.4 Mpa as an example (Table 1), it can be seen that σ_1 and σ_3 reduce, and σ_2 enhances gradually in the process of increasing the stress Lode's angle θ_σ from -30° to 30° (Fig. 4). The value of σ_2 increases from that of σ_3 to that of σ_1. The controlled values by the true triaxial apparatus are very close to the calculated values using Equations (2)-(4), suggesting the servo loading system of the apparatus is reliable. In the three true triaxial tests, the variations in principal stresses are unanimous, as shown in Fig. 5. Note that the test CPQ3 with constant deviatoric stress q=0.6 Mpa was terminated as the specimen failed when θ_σ achieved 30° in the first cycle.

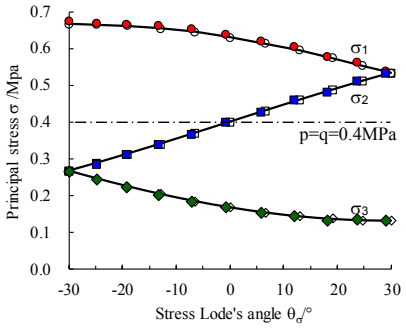

Figure 4. Comparison between controlled and calculated values of three principal stresses

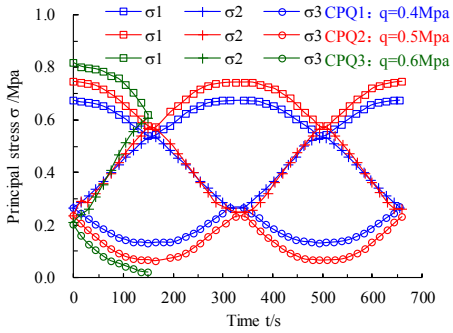

Figure 5. Variations in three principal stresses with testing time

When soil experiences repeated loading and unloading cycles, a hysteresis loop forms in each cycle. The hysteresis width gets

narrower gradually until that no plastic deformation occurs, indicating perfectly elastic deformation. In the CPQ tests, material behavior in the increasing and decreasing processes of the stress Lode's angle is similar with that in the above loading and unloading tests. In the tests CPQ1 and CPQ2, the volumetric and deviatoric strains show small hysteresis loops in the first descending process and the second varying cycle of stress Lode's angle (Figures 6a and 7a), indicating that soil deformation should be primarily elastic. Accordingly, the greater deformation should be elastoplastic in the first rising process of the stress Lode's angle.

In the test CPQ1, the deviatoric strain increases consistently and achieves its peak value of 2.1% as the stress Lode's angle grows from -30° to 30° in its first rising process (Fig. 6a). It then decreases gradually to 1.5% as the stress Lode's angle reduces from 30° to -30°. In the second rising and descending cycle of the stress Lode's angle, the deviatoric strain demonstrates obvious hysteresis. It increases to 2.2% firstly, and then drops to 1.7%. Similarly, the volumetric strain enhances to 0.44% with the rising stress Lode's angle, and then enhances further to 0.60% with the descending stress Lode's angle (Fig. 7a). Careful examination suggests the former increase should include both elastic and plastic deformation, while the latter should be mainly elastic deformation. In the second increasing and decreasing cycle of the stress Lodes's angle, the volumetric strain reduces to 0.58% firstly, and then enhances to 0.67%.

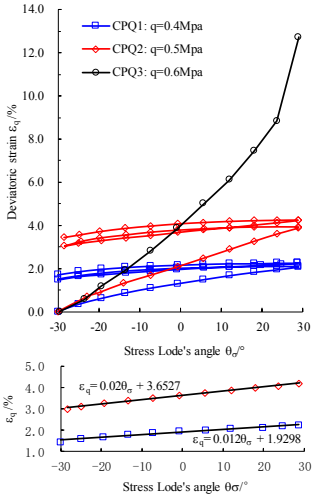

Figure 6. (a) Variation in the deviatoric strain with the stress Lode's angle; (b) the linear regression line in the second rising process of the stress Lode's angle

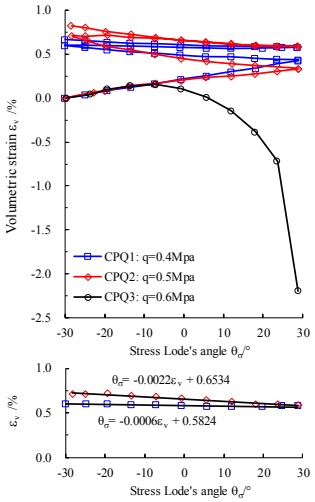

Figure 7. (a) Variation in the volumetric strain with the stress Lode's angle; (b) the linear regression line in the second rising process of the stress Lode's angle

In the test CPQ2, the specimen shows consistent deformation with that in CPQ1. The deviatoric strain rises continuously and reached the peak value 3.9% in the firsting rising process of the stress Lode's angle. Thereafter, the deviatoric strain reduces to 3.0% with the decrease of the stress Lode's angle from 30° to -30°. In the second increasing and decreasing cycle of the stress Lode's angle, the deviatoric strain demonstrates a small hysteresis loop. It increases to 4.2% firstly, and then drops to 3.4% (Fig. 6a). The volumetric strain increases to 0.34% with the increasing stress Lode's angle, indicating elastic and plastic deformation. It increases further to 0.72% with the decreasing stress Lode's angle, indicating dominated elastic deformation (Fig. 7a). In the second varying cycle of the stress Lodes's angle, the volumetric strain reduces to 0.60% firstly, and then enhances to 0.84%.

Being similar to phenomena in a typical repeated loading and unloading test, the deviatoric and volumetric strain curves in the tests CPQ1 and CPQ2 are roughly parallel in the first and second decreasing processes of stress Lode's angle (Figures 6 and 7). Between them, the deforming curves in the second rising process should be elastic, and are replotted and best-fitted using a linear regression form in Figures 6b and 7b. The values of the elastic deformaton parameters can be obtained from the slopes of the deviatoric strain curves (0.02 and 0.012, respectively) and that of the volumetric strain curves (-0.0022 and -0.0006, respectively).

In the test CPQ3, the specimen accelerated deformed with the increasing stress Lode's angle and finally reached failure state (Fig. 6a). When the angle value approaches 30°, both the deviatoric and volumetric strains develop rapidly and achieve 12.7% and -2.2%, respectively. There is a small difference in the initial slope of the deviatoric strain curves, which suggests that the initial modulus seems to be affected by the q/p stress ratio (Fig. 6a).

4 DISCUSSION

4.1 *Strain components*

In granular materials' elastoplastic constitutive models, the stress-strain relationship is commonly expressed in incremental forms below:

$$d\varepsilon_v = A_1 dp + A_2 dq \tag{7}$$

$$d\varepsilon_q = B_1 dp + B_2 dq \tag{8}$$

where $d\varepsilon_v$ is the volumetric strain increment; $d\varepsilon_q$ is the deviatoric strain increment; A_1 and A_2 are the coefficients of the mean and deviatoric stress increments related to the volumetric strain increment; B1 and B2 are the coefficients of the mean and deviatoric stress increments related to the deviatoric strain increment.

Following Equations (7)-(8), it is clearly that neither deviatoric strain nor volumetric strain occur when the mean and deviatoric stresses maintain constants. The above equations cannot reflect the effects of the stress Lode's angle θ_σ on soil deformation. They include inadequate assumptions and are lack of scientific basis and experimental verification. As presented in Figures 6 and 7, obvious elastic and plastic deformation can be observed under constant mean and deviatoric stresses. The εv:εq strain paths of the three tests are further demonstrated in Fig. 8. The volumetric strain enhances consistently with the deviatoric strain, suggesting compression of soil specimen in the tests CPQ1 and CPQ2. In CPQ3, the volumetric strain increases slightly and then accelerated decreases, suggesting soil compression followed by swelling.

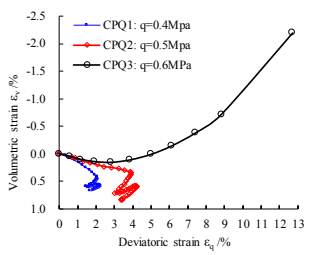

Figure 8 The ε_v:ε_q strain paths

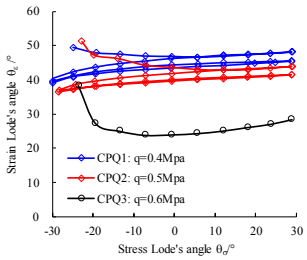

Figure 9. Variations in the strain Lode's angle with the stress Lode's angle

As mentioned previously, the unique varied stress component is the stress Lode's angle. A more reasonable approach is incorporating the increment of the stress Lode's angle into the volumetric and deviatoric strain increments expressions (Equations (7)-(8)).

$$d\varepsilon_v = A_1 dp + A_2 dq + A_3 d\theta_\sigma \tag{9}$$

$$d\varepsilon_q = B_1 dp + B_2 dq + B_3 d\theta_\sigma \tag{10}$$

where A_3 and B_3 are the coefficients of the stress Lode's angle related to the volumetric and deviatoric strain increments.

4.2 *Anisotropy*

Being similar to stress components, three strain components are necessary to depict a point in the strain space, a common form of which is the principal strains (ε_1, ε_2, ε_3). In the strain space, a strain deviatoric plane and the strain π plane are parallel. The distance ε_m between them is the truncated length along the isocline, i.e. one third of the volumetric srain ε_v. The vector length ε_r defines the distance from the origin projection to a certain strain state in the deviatoric plane. On the basis of Equations (5)-(6), two sets of strain parameters (ε_v, ε_q) and (ε_m, ε_r) are fully associated and can be expressed below:

$$\varepsilon_r/\varepsilon_m = \lambda \cdot \varepsilon_q/\varepsilon_v = \sqrt{27/2} \cdot \varepsilon_q/\varepsilon_v \approx 3.674 \cdot \varepsilon_q/\varepsilon_v \tag{11}$$

where λ is the conversion factor, $\lambda \approx 3.674$.

Two strain components ε_v and ε_q are commonly adopted in soil's elastoplastic constitutive models, however, the third strain component is still in absence to accurate determine a certain strain state. To avoid related assumptions in constitutive models, the strain Lode's angle θ_ε should be taken into account:

$$tan\theta_\varepsilon = (2\varepsilon_2 - \varepsilon_1 - \varepsilon_3)/[\sqrt{3}(\varepsilon_1 - \varepsilon_3)] \tag{12}$$

Three strain components (ε_v, ε_q, θ_ε) are adopted in this section to determine strain state in the strain space. Being similar with other two strain components, the strain Lode's angle shows clear hysteresis in the rising and descending cycles of the stress Lode's angle as well (Fig. 9). The deviatoric strain is normalized using the volumetric strain, and then shown in the strain deviatoric plane together with the strain Lode's angle θ_ε in Fig. 10. The conversion factor λ is reserved for the plotted strain states, which remains consistent with the strain space determined by three principal strain axes. In the tests CPQ1 and CPQ2, when the stress Lode's angle varies within -30°~30° in the first sector I, the strain Lode's angle varies within 39°~49° and 37°~51° in the second sector II, respectively. The differences in the directions of principal stresses and strains indicate the anisotropic characteristics of soil specimens. Specimen preparation in laboratory neeeds repeated vertical compaction under lateral confining condition. Similarly, rockfill material needs to be compacted via repeated static and dynamic rolling in dam construction. The above experimental and field approaches inevitably lead to the formation of anisotropic geological element.

The noncoaxial behavior of granular material has been reported by Lashkari and Latifi (2008), which implies that the directions of principal strains are different with that of principal stresses and reflects material's anisotropy. The direction of a certain principal strain increment should be between the direction of the corresponding principal stress and the direction of its increment. The strain Lode's angle is greater than 30° in the tests CPQ1 and CPQ2, suggesting non-coaxial characteristics. In the test CPQ3, the strain Lode's angle θ_ε drops fast from 38° to 24°, and then increases gradually to roughly 29° when the stress Lode's angle θ_σ achieves 30° at the end of the test (Fig. 9c), indicating coaxial tendency at failure state. The above coaxial feature was reported by Hu et al. (2017) based on their hollow cylinder tests as well.

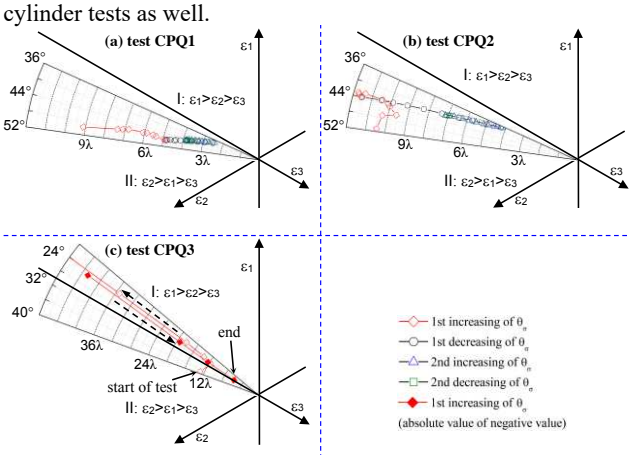

Figure 10. Strain paths in the strain deviatoric plane in constant p and q test

4.3 *Dilatancy*

The material dilatancy is defined as the ratio of plastic volumetric strain increment to plastic deviatoric strain increment.

$$D = d\varepsilon_v^p / d\varepsilon_q^p = (d\varepsilon_v - d\varepsilon_v^e)/(d\varepsilon_q - d\varepsilon_q^e) \tag{13}$$

where the superscripts 'e' and 'p' stands for 'elastic' and 'plastic', respectively.

Soil deformation is further analyzed in incremental form by applying eq. (13) to examine the dilatancy behavior of the rockfill material. The plastic volumetric and deviatoric strain increments are obtained by deducting elastic strain increments from total strain increments. In CPQ1 and CPQ2, the material deformation should be elastoplastic and elastic in the first and second rising processes of θ_σ, respectively. In CPQ3, elastic strain increments are estimated using average slope values in Figures 6b and 7b and applied to calculation of plastic strain increments. All the three specimens show contractive behavior at the test beginning, and demonstrate deviation as deformation increases (Fig. 11). The initial dilatancy at θ_σ=-30° (i.e. b=0, or σ_2=σ_3) reduces with the increase of q/p stress ratio in the three tests. The above tendency has been widely reported under axisymmetric stress condition for loose cohesionless material (e.g., Li and Dafalias 2000). With the increase of the stress Lode's angle, the dilatancy enhances consistently in the test CPQ1, fluctuates slightly in the test CPQ2, and decreases continuously from positive to negative values in CPQ3. The above phenomena reflects that the volumetric behavior is contraction in the tests CPQ1 and CPQ2, and transforms from contraction to dilation in the test CPQ3.

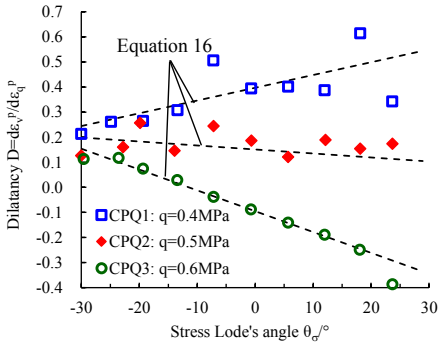

Figure 11. Variations in the dilatancy with the stress Lode's angle and the fitting lines using the proposed dilatancy equation

5 CONCLUSION

A self-developed large-scale true triaxial apparatus with a special low-friction technique was adopted to perform constant mean and deviatoric stresses tests on a rockfill material. Its behavior with the independent variation of stress Lode's angle from -30° to 30° was investigated under different q/p stress ratios. The following conclusions can be drawn from this study.

(1) Soil deforms together with the variation of the stress Lode's angle under the condition of constant mean and deviatoric stresses. There is a small difference in the initial slope of the deviatoric strain curves, which suggests that the initial modulus seems to increase as the q/p stress ratio grows.

(2) Elastoplastic strains occur in the first increasing process of the stress Lode's angle. In the following decreasing, increasing and decreasing processes, hystereses can be observed for the deviatoric strain, the volumetric strain, and the strain Lode's angle, the last of which is needed to determine a point in the strain space and should be contained in rockfill material's constitutive model.

(3) Being affected by initial q/p stress ratio, the rockfill material could reach failure state with the increasing stress Lode's angle. Following the constant mean and deviatoric stresses path, a specimen shows non-coaxial characteristics prior to failure, and tends to be coaxial at failure state.

6 ACKNOWLEDGEMENTS

The authors acknowledge the financial support of the National Natural Science Foundation Projects of China (Grants No. 51979010, No. U1765203) and the Basic Research Project for Central Public Research Institutes (Grant No. CKSF2019182/YT).

7 REFERENCES

Gibson R.E. and Henkel D.J. 1954. Influence of duration of tests at constant rate of strain on measured "drained" strength. *Géotechnique* 4 (1), 6-15.

Darcy H. 1856. *Les fontaines publiques de la ville de Dijon*. Dalmont, Paris.

Terzaghi K. 1936. The shearing resistance of saturated soils. *Proc. 1st Int. Conf. Soil Mech.*, Cambridge, Mass., 1, 54-56.

Anhdan, L. Q., Koseki, J., and Sato, T. 2006. Evaluation of quasi-elastic properties of gravel using a large-scale true triaxialapparatus. Geotechnical Testing Journal, 29(5): 374-384.

Anantanasaku, P, Yamamuro, J. A., and Lade, P. V. 2012. Three-dimensional drained behavior of normally consolidated anisotropic kaolin clay[J]. Soils and Foundations, 52(s1): 146-159.

Cheng, Z., Wang, Y., Rao, X., et al. 2015. The bidirectional low-friction loading plate for the true triaxial apparatus[P]. Chinese Patent No.: ZL 201520613876, China.

Choi, C., Arduino, P. and Hardney, M.D. 2008. Development of a true triaxial apparatus for sands and gravels[J]. Geotechnical Testing Journal, 31(1): 32-44.

Guo, P., and Su, X. 2007. Shear strength, interparticle locking, and dilatancy of granular materials[J]. Canadian Geotechnical Journal, 44(5): 579-591.

Honkanadavara, N.P., and Sharmab, K.G. 2016. Modeling the triaxial behavior of riverbed and blasted quarried rockfill materials using hardening soil model[J]. Journal of Rock Mechanics and Geotechnical Engineering, 8(3): 350-365.

Hu, P., Wei, C., Yang, L. et al. 2017. Non-coaxial Behavior of Sands in Fixed Principal Stress Axes Shear Tests[J]. Journal of University of Jinan (Science and Technology), 31(06):478-484.

Indraratna, B., Ionescu, D., and Christie, H. D. 1998. Shear behavior of railway ballast based on large-scale triaxial tests[J]. Journal of geotechnical and geoenvironmental Engineering, 124(5): 439-449.

Lade, P.V., and Wang, Q. 2001. Analysis of shear banding in true triaxial tests on sand[J]. Journal of Engineering Mechanics, 127(8): 762-768.

Lashkari, A., and Latifi, M. 2008. A non-coaxial constitutive model for sand deformation under rotation of principal stress axes[J]. International Journal for Numerical and Analytical Methods in Geomechanics, 32(9): 1051-1086.

Li, X.S., and Dafalias, Y.F. 2000. Dilatancy for cohesionless soils[J]. Geotechnique, 50(4): 449-460.

Ministry of Water Resources of the PRC, China. 1999. Specification of Soil Test (SL237—1999) [S]. Beijing: China Water and Power Press.

Rowe, P. W. 1962. The stress-dilatancy relation for static equilibrium of an assembly of particles in contact. Proc. R. Soc., London, Ser. A. 269: 500-527.

Shi, W.C, Zhu, J.G., Dai, G.Z., et al. 2015. True triaxial tests on influence of spherical and deviatoric stresses on deformation of coarse-grained soil[J]. Chinese Journal of Geotechnical Engineering, 37(5): 776-783.

Sun, D.A., Huang, W.X., and Yao, Y.P. 2008. An experimental study of failure and softening in sand under three-dimensional stress condition, Granular Matter, 10(3), 187-195.

Taiebat, M., and Dafalias, Y. F. 2008. SANISAND: Simple anisotropic sand plasticity model[J]. International Journal for Numerical and Analytical methods in geomechanics, 32(8): 915-948

Wan, R.G., and Guo, R. G. 1998. A simple constitutive model for granular soils: modified stress-dilatancy approach[J]. Computers and Geotechnics, 22(2): 109-133.

Wood, D. M. 1990. Soil behaviour and critical state soil mechanics. New York: Cambridge University Press.

Xiao, Y., Liu, H.L., Zhu, J.G. et al. 2011. Dilatancy equation of rockfill material under the true triaxial stress condition[J]. Science China Technological Sciences, 54(s1):175-184.

Xiao, Y., Liu, H.L., Sun, Y. et al. Stress–dilatancy behaviors of coarse granular soils in three-dimensional stress space[J]. Engineering Geology, 2015, 195: 104-110.

Xiao Y., Sun Y., Liu H. et al. 2016. Critical state behaviors of a coarse granular soil under generalized stress conditions[J]. Granular Matter, 18(2): 1-13.

Yin, J.H., Cheng, C.M., Kumruzzaman, M. et al. 2010. New mixed boundary, true triaxial loading device for testing three-dimensional stress–strain–strength behaviour of geomaterials. Canadian Geotechnical Journal, 47(1): 1-15.

Zhou, Y.F. , Pan, J.J. , Cheng, Z.L. et al. 2017. Strength and dilation of sandy gravel material based on large-scale true triaxial tests[J]. Chinese Journal of Rock Mechanics and Engineering, 36(11): 2818-2825.